

are expected to be primarily Pt(5d_{z²}), these levels in [Pt₂(pop)₄X₂]⁴⁻ may contain substantial contributions from π(P₂O₃H₂) and possibly (p_z, s) metal orbitals.²⁰

Axial σ-electronic delocalization will be enhanced in [Pt₂(pop)₄X₂]⁴⁻ complexes in which the energies of dσ and σ(X) orbitals are not very different. In this circumstance, the σ → σ* transition is no longer Pt₂ localized, and therefore its energy should not necessarily be related in any simple way to Pt-Pt bond strength.^{4b} While decreasing values of E(σ → σ*) in diplatinum(III,III) diphosphite bridged complexes generally correlate with increasing Pt-Pt bond distances (Table VIII), axial LMCT mixing selectively affects E(σ → σ*) in certain cases. For example, the Pt-Pt bond distances in [Pt₂(pop)₄(NO₂)₂]⁴⁻ and [Pt₂(pop)₄(SCN)₂]⁴⁻ differ by only ~0.006 Å, but E(σ → σ*) of the latter ion is red shifted by ~2400 cm⁻¹ from that of the nitro complex. Also, the very high E(σ → σ*) of [Pt₂(pop)₄-

(Im)₂]⁴⁻ relative to the transition energies of complexes with similar Pt-Pt distances undoubtedly reflects the Pt₂-localized nature of σ → σ* with Im⁻ as the axial ligand.

Acknowledgment. We thank Vince Miskowski for helpful discussions. This research was supported by the Committee of Conference and Research Grants of the University of Hong Kong (C.-M.C. and W.M.L.) and National Science Foundation Grant CHE82-18502 (H.B.G.). Wai-Man Lee acknowledges a graduate studentship from the Croucher Foundation.

Registry No. 1, 102614-74-4; 2, 102630-07-9; 3, 102614-75-5; K₂[Pt₂(pop)₄(py)₂], 102614-76-6; K₂[Pt₂(pop)₄(nicot)₂], 102614-77-7; [Bu₄N]₄[Pt₂(pop)₄], 102630-09-1; K₄[Pt₂(pop)₄], 79716-40-8; Pt, 7440-06-4.

Supplementary Material Available: Imidazolyl H coordinates, anisotropic temperature factors, and structure factor tables for 1-3 (62 pages). Ordering information is given on any current masthead page.

(20) Rice, S. F.; Gray, H. B. *J. Am. Chem. Soc.* 1983, 105, 4571-4575.

Excited-State Spectra and Lifetimes of Quadruply Bonded Binuclear Complexes: Direct Observation of a New Transient Species following Decay of the ¹(δδ*) State in Mo₂Cl₄(PBu₃)₄

Jay R. Winkler,*[†] Daniel G. Nocera,[‡] and Thomas L. Netzel*^{†,§}

Contribution from the Department of Chemistry, Brookhaven National Laboratory, Upton, New York 11973, and Department of Chemistry, Michigan State University, East Lansing, Michigan 48824. Received August 15, 1985

Abstract: This paper reports transient absorption kinetics studies in the 10⁻¹¹-10⁻³ s time range for [Re₂Cl₈]²⁻ (I), [Mo₂Cl₈]⁴⁻ (II), Mo₂Cl₄(CH₃CN)₄ (III), and Mo₂Cl₄(PBu₃)₄ (IV) in solution at room temperature. A detailed description of the optical layout and equipment used to measure the kinetics in the 10⁻⁸-1 s time range following picosecond excitation is also given. Complexes I-III have small steric barriers to rotation about the M-M bond and upon photoexcitation appear to form ¹(δδ*)_{staggered} metal-metal charge-transfer (MMCT) states in <20 ps. The absorption spectra of ¹(δδ*) MMCT states are shown to have characteristic, strong charge-transfer (CT) bands in the near UV. Complex IV has bulky alkylphosphine groups and should retain its eclipsed geometry in its ¹(δδ*) excited state in noncoordinating solvents. In CH₃CN, IV undergoes some nuclear relaxation in the ¹(δδ*) state with a rate constant of 10⁹ s⁻¹. A particularly important result is that in complex IV a nonluminescent transient species is observed at long times (τ ~ 100 ns) following the decay of the ¹(δδ*) MMCT state.

The study of metal-metal bonding in binuclear complexes continues to be an active area of research in inorganic chemistry.¹⁻⁴ An important subset of binuclear complexes pairs two dⁿ transition metals in molecules described by ground states with metal-metal quadruple bonds. Numerous experimental³ and theoretical⁴ studies have clarified important aspects of the electronic structures of these molecules, but many fundamental questions remain unanswered.

A simple molecular orbital scheme for dⁿ-dⁿ [M₂X₈]ⁿ⁻ complexes with D_{4h} symmetry is illustrated in Figure 1. The eight d-electrons from the two metals fill the four metal-metal bonding orbitals to produce a (σ²π⁴δ²) ground-state configuration and a quadruple bond. This model correctly predicts a diamagnetic ground state for these molecules and an eclipsed (D_{4h}) ligand conformation. It further predicts that a spin and dipole allowed δ² → ¹(δδ*) excitation should be apparent in the absorption spectra of these molecules. Indeed, bands between 500 and 700 nm in the visible spectra of these molecules have been assigned to this ¹A_{1g} → ¹A_{2u} transition.³ The absorption bands are polarized

Table I. State Orderings in dⁿ-dⁿ Complexes: [Re₂Cl₈]²⁻

E ^a , eV	states
2.6	³ A _{2u} (ππ*)
2.6	¹ E _g (πδ*)
2.2	¹ A _{1g} (δδ*): ¹ [(xy _A)(xy _A) + (xy _B xy _B)]
1.8	¹ A _{2u} (δδ*): ¹ [(xy _A)(xy _A) - (xy _B xy _B)]
1.8	³ E _g (πδ*)
0.4	³ A _{2u} (δδ*): ³ [(xy _A)(xy _B)]
0	¹ A _{1g} : ¹ [(xy _A)(xy _B)]

^aReference 4c.

parallel to the M-M bond (molecular z-axis) and at low temperature resolve into vibrational progressions in the M-M

(1) Cotton, F. A.; Walton, R. A. *Multiple Bonds Between Metal Atoms*; Wiley: New York, 1982.

(2) Chisholm, M. H.; Cotton, F. A. *Acc. Chem. Res.* 1978, 11, 356.
 (b) Cotton, F. A. In *Transition Metal Chemistry, Procedure Workshop*; Müller, A.; Diemann, E., Eds.; Verlag Chem: Weinheim, Germany, 1981; p 51. (c) *Reactivity of Metal-Metal Bonds*; Chisholm, M. H., Ed. ACS Symposium Series; American Chemical Society: Washington, DC 1981; Vol. 155. (d) Chisholm, M. H.; Rothwell, I. P. *Prog. Inorg. Chem.* 1982, 29, 1. (e) Chisholm, M. H. *Polyhedron* 1983, 2, 681. (f) Meyer, T. J.; Caspar, J. V. *Chem. Rev.* 1985, 85, 187.

[†] Brookhaven National Laboratory.

[‡] Michigan State University.

[§] Present Address: Amoco Corporation, Corporate Research Department, Amoco Research Center, Post Office Box 400, Naperville, IL 60566.

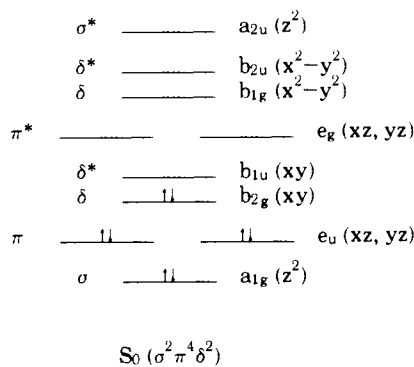


Figure 1. Relative energies of molecular orbitals arising from metal *d*-orbital interactions in a quadruply bonded $[M_2X_8]^{n+}$ complex. The molecule has D_{4h} symmetry with the *z*-axis along the M–M bond, and the *x*- and *y*-axes are parallel to the M–X bonds. Each molecular orbital is labeled according to its bond type, symmetry, and *d*-orbital parentage.

stretching mode. These progressions indicate an increase in the M–M separation due to the absence of a δ -bond in the $^1(\delta\delta^*)$ excited state. A further consequence of this δ -bond rupture is that, in the absence of opposing steric interactions, the *staggered* conformation is believed to be more stable in the $^1(\delta\delta^*)$ excited state.^{3g,4c} This situation is entirely analogous to that encountered in simple olefins where, in $(\pi\pi^*)$ excited states, the molecules adopt a twisted rather than planar geometry.⁵ As with simple olefins, the effects of this excited state conformational change should be manifested in luminescence and decay properties.

Though conceptually quite appealing, the molecular orbital model does not provide an accurate quantitative picture of the electronic structure of quadruply bonded metal dimers, especially in terms of δ -bonding. The poor overlap of the d_{xy} orbitals involved in δ -bonding is in large part responsible for the errors in these calculations and suggests that a valence bond description of the electrons in these orbitals would be more appropriate. Such an approach was used in an *ab initio* calculation of the $Re_2Cl_8^{2-}$ electronic structure, some of the results of which are outlined in Table I.^{4c} In the valence bond model, the $^1A_{1g}$ ground state has one electron in each d_{xy} orbital. At slightly higher energy (0.4 eV) is the $^3A_{2u}$ excited state, which still has one electron in each d_{xy} orbital, though now triplet paired. This state correlates with the $^3(\delta\delta^*)$ excited state of the molecular orbital model. Lying much higher in energy are two ionic singlet excited states that arise from antisymmetric ($^1A_{2u}$, 1.8 eV) and symmetric ($^1A_{1g}$, 2.2 eV) combinations of configurations with both d_{xy} electrons on one metal center. These two states correlate with the $^1(\delta\delta^*)$ and $^1(\delta^2)$ molecular orbital configurations, respectively. An important feature of this model is that it correctly predicts a large $^1A_{2u} - ^3A_{2u}$ energy gap and a relatively small separation between the ground state and the $^3A_{2u}$ level.⁶ Within this manifold of four

states, the only spin and dipole allowed transition from the $^1A_{1g}$ ground state is to the $^1A_{2u}$ excited state, which corresponds to a metal-to-metal charge transfer (MMCT) transition and correlates with the $\delta^2 \rightarrow ^1(\delta\delta^*)$ excitation. An interesting aspect of the *ab initio* calculation on $Re_2Cl_8^{2-}$ is the prediction that the $^3E_g(\pi\delta^*)$ state is nearly degenerate with the $^1A_{2u}$ level. The presence of such a state could have important ramifications in the photophysics of these molecules.

The lowest energy, and now least controversial, absorption feature in the electronic spectra of these quadruply bonded molecules is the band assigned to the $^1A_{1g} \rightarrow ^1A_{2u}[\delta^2 \rightarrow ^1(\delta\delta^*)$ or MMCT] excitation.⁷ The general agreement about this absorption band is in contrast to the uncertainty surrounding the luminescence band that maximizes just to the red of this absorption feature in many of these molecules. Complexes such as $[Re_2Cl_8]^{2-}$, $[Re_2Br_8]^{2-}$, and $[Mo_2Cl_8]^{4-}$ do not exhibit mirror image absorption and emission spectra.^{3b,4} The radiative rate constants calculated from luminescence yields and lifetimes are 10^4 times lower than those determined from the $\delta^2 \rightarrow ^1(\delta\delta^*)$ absorption profiles.^{3b} Recently, vibrational structure has been observed in the 10 K emission spectrum of $K_4[Mo_2Cl_8]$.³ⁱ The apparent origins of the absorption and emission bands do not overlap ($\Delta E \sim 600 \text{ cm}^{-1,3c}$), and progressions in the Mo–Cl stretching vibration are found in emission while Mo–Mo vibrational progressions appear in the $\delta^2 \rightarrow ^1(\delta\delta^*)$ absorption band.

Two explanations have been proposed to account for the lack of mirror-image absorption and emission spectra in $[M_2X_8]^{n+}$ complexes. A detailed analysis of the luminescence spectra of $K_4Mo_2Cl_8$ at 10 K has led to the suggestion that the emitting state is not $^1A_{2u}(\delta\delta^*)$ but rather a 3E_g or $^3A_{2g}$ state.³ⁱ An alternative proposal for the anomalous luminescence behavior is that absorption transitions in $[M_2X_8]^{n+}$ complexes such as $[Re_2Cl_8]^{2-}$ produce $^1A_{2u}(\delta\delta^*)$ MMCT states with eclipsed geometry, while the emission originates from $^1(\delta\delta^*)$ MMCT states of staggered (D_4 or D_{4d}) geometry (*vide supra*).^{3b} The poor Franck–Condon overlap and reduced transition dipole for this latter transition would produce a broad, weak emission band. The presence of Mo–Cl vibrational progressions in the emission spectrum of $Mo_2Cl_8^{4-}$, rather than the Mo–Mo progressions found in absorption, could arise from differences in the coupling of the vibrational modes to the two electronic transitions: $^1(\delta^2)_{\text{eclipsed}}^2 \rightarrow ^1(\delta\delta^*)_{\text{eclipsed}}$; $^1(\delta\delta^*)_{\text{staggered}} \rightarrow ^1(\delta^2)_{\text{staggered}}$.

In support of the second hypothesis are the spectra of $Mo_2X_4(PR_3)_4$ complexes ($X = Cl, Br, I; R = \text{alkyl}$). The emission bands in these molecules are mirror images of their $\delta^2 \rightarrow ^1(\delta\delta^*)$ absorption profiles and at low temperature resolve into vibrational progressions in the Mo–Mo stretching mode.^{3b,8} The bulky phosphine ligands in these quadruply bonded Mo dimers are believed to create a large steric barrier to rotation about the metal–metal bond. Hence, the $^1(\delta\delta^*)$ excited state is likely to retain the eclipsed ground state geometry and produce well-behaved luminescence.

We have undertaken a transient absorption spectroscopic study of the excited-state dynamics in a series of quadruply bonded metal dimers. This paper is a report on results from $[Re_2Cl_8]^{2-}$ (I), $[Mo_2Cl_8]^{4-}$ (II), $Mo_2Cl_4(CH_3CN)_4$ (III), and $Mo_2Cl_4(PBu_3)_4$ (IV) in solution at room temperature.

Experimental Section

Kinetics and Spectral Measurements. Difference spectra and kinetics as well as emission lifetimes were recorded after photoexcitation by a single pulse from a Nd/YAG laser system. The Nd/YAG laser was actively and passively mode-locked. The laser's output was spatially filtered both within the oscillator cavity and between the first and second amplifiers to ensure a smoothly varying spatial energy distribution within each pulse. A detailed description of the system used in the 10^{-11} – 10^{-8}

(3) (a) Cowman, C. D.; Gray, H. B. *J. Am. Chem. Soc.* **1973**, *95*, 8177. (b) Cotton, F. A.; Martin, D. S.; Fanwick, P. E.; Peters, T. J.; Webb, T. R. *J. Am. Chem. Soc.* **1976**, *98*, 4681. (c) Fanwick, P. E.; Martin, D. S.; Cotton, F. A.; Webb, T. R. *Inorg. Chem.* **1977**, *16*, 2103. (d) Cowman, C. D.; Trogler, W. C.; Gray, H. B. *Isr. J. Chem.* **1977**, *15*, 308. (e) Trogler, W. C.; Cowman, C. D.; Gray, H. B.; Cotton, F. A. *J. Am. Chem. Soc.* **1977**, *99*, 2993. (f) Trogler, W. C.; Gray, H. B. *Acc. Chem. Res.* **1978**, *11*, 232. (g) Miskowski, V. M.; Goldbeck, R. A.; Klinger, D. S.; Gray, H. B. *Inorg. Chem.* **1979**, *18*, 86. (h) Rice, S. F.; Wilson, R. B.; Solomon, E. I. *Inorg. Chem.* **1980**, *19*, 3425. (i) Fraser, I. F.; Peacock, R. D. *Chem. Phys. Lett.* **1983**, *98*, 620. (j) Clark, R. J. H.; Stead, M. J. *Inorg. Chem.* **1983**, *22*, 1214. (k) Manning, M. C.; Trogler, W. C. *J. Am. Chem. Soc.* **1983**, *105*, 5311. (l) Martin, D. S.; Huang, H.-W.; Newman, R. A. *Inorg. Chem.* **1984**, *23*, 699. (m) Robbins, G. A.; Martin, D. S. *Inorg. Chem.* **1984**, *23*, 2086. (n) Huang, H.-W.; Martin, D. S. *Inorg. Chem.* **1985**, *24*, 96. (o) Fanwick, P. E. *Inorg. Chem.* **1985**, *24*, 258. (p) Fanwick, P. E.; Bursten, B. E.; Kaufmann, G. B. *Inorg. Chem.* **1985**, *24*, 1165. (q) Dallinger, R. F. *J. Am. Chem. Soc.* **1985**, *107*, 7202.

(4) (a) Mortola, A. P.; Moskowitz, J. W.; Rösch, N.; Cowman, C. D.; Gray, H. B. *Chem. Phys. Lett.* **1975**, *32*, 283. (b) Norman, J. G.; Kolari, H. J. *J. Am. Chem. Soc.* **1975**, *97*, 33. (c) Hay, P. J. *J. Am. Chem. Soc.* **1982**, *104*, 7007. (d) Mathisen, K. B.; Wahlgren, U.; Pettersson, L. G. M. *Chem. Phys. Lett.* **1984**, *104*, 336. (e) Strömberg, A.; Pettersson, L. G. M.; Wahlgren, U. *Chem. Phys. Lett.* **1985**, *118*, 389.

(5) Merer, A. J.; Mulliken, R. S. *Chem. Rev.* **1969**, *69*, 639.

(6) Hopkins, M. D.; Zietlow, T. C.; Miskowski, V. M.; Gray, H. B. *J. Am. Chem. Soc.* **1985**, *107*, 510.

(7) Recently however this assignment in $Mo_2Cl_8^{4-}$ has been questioned.^{4d,e}

(8) (a) Hopkins, M. D.; Gray, H. B. *J. Am. Chem. Soc.* **1984**, *106*, 2468. (b) Zietlow, T. C.; Hopkins, M. D.; Gray, H. B. *J. Solid State Chem.* **1985**, *57*, 112.

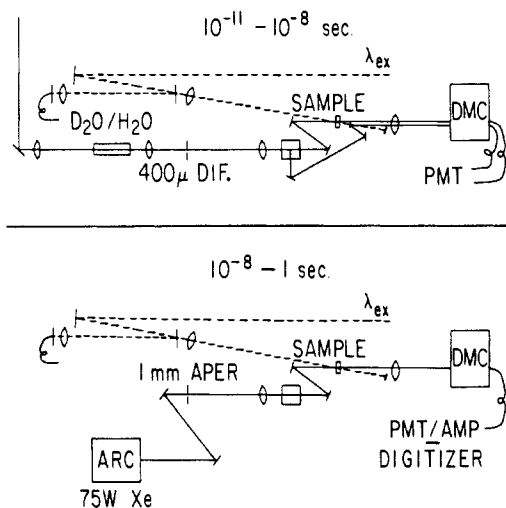


Figure 2. Optical layouts for short time (upper) and long time (lower) transient absorption spectroscopic experiments: D_2O/H_2O , 10-cm path length cell containing a mixture of D_2O and H_2O (80:20 by volume); 400 μ DIF, 400- μ m aperture in contact with a glass diffuser; SAMPLE, 2-mm path length cell; DMC, double $1/4$ -m monochromator; PMT, photomultiplier tubes; 75 W Xe ARC, current-pulsed 75-W xenon arc lamp; 1-mm APER, 1-mm-diameter aperture; PMT/AMP DIGITIZER, photomultiplier tube signal fed into a quasidifferential amplifier then into a CAMAC-controlled LeCroy TR8828B transient digitizer (see text).

s range has been presented elsewhere, and only highlights are reported here.⁹

In the 10^{-11} – 10^{-8} s range (top of Figure 2), picosecond-duration probe light is generated in a 10-cm cell of D_2O and H_2O . Kinetics are measured with a pulse-and-probe procedure with the difference in time between the excitation-pulse and probe-pulse determined by an optical delay line (not shown). The instrument response time under these conditions is 20–25 ps. Every data point is plotted with its corresponding statistical error. This error is the standard deviation of the mean of 50 independent change in absorbance (ΔA) measurements. All ΔA measurements were made within a specified range of photoexcitation energies. Data from excitation pulses outside the allowed range were not used. All samples were tested for multiphoton artifacts by varying the photoexcitation energy. The reported difference spectra and kinetics were measured at photoexcitation energies below the empirically determined onset of multiphoton products.

The time range for viewing transient absorption produced by picosecond excitation was extended for this work to cover the 10^{-8} –1 s range (bottom of Figure 2). In this case, the probe light is of much longer duration (1–4 ms or cw), and the kinetics are measured in real time with a CAMAC-controlled transient digitizer. In order to compensate for the low probe light collection efficiency of our F/15 optical layout, three changes are made for extended time scale measurements. First, a 1-mm diameter probe aperture *without* a diffuser plate is used, in contrast to a 400- μ m diameter aperture *with* a diffuser plate in the short (10^{-11} – 10^{-8} s) time range experiments. Second, a larger (~ 3 -mm diameter) photoexcitation spot is used to accommodate the larger probe spot in the sample cell. Third, a dummy beam splitter with high transmission replaces the 70/30 (T/R) cube beam splitter necessary in the short time range.

The 75-W xenon lamp and power supply were manufactured by Photon Technology International of Princeton, NJ. The lamp's reflector was constructed to focus at F/15 in order to match our picosecond laser system's optical layout (lamp model 02-A1000S-F15, power supply 02-LPS1000, lamp starter 02-LPS-001). For intermediate time range measurements (10^{-8} – 10^{-5} s), the xenon lamp was pulsed to ~ 30 A for 1–4 ms with a 2-Hz maximum repetition rate. For longer lived transients the lamp was run cw at ~ 40 W.

The detector was a Hamamatsu R928 photomultiplier tube wired for five stage operation and linear to within 1% up to 10 mA for a 5-ms pulse of light (data supplied by Yuji Shinoda, Hamamatsu Corp. of Middlesex, NJ). The quasidifferential amplifier (rise time 2.5 ns with no overshoot or ringing) was designed and built by Lee Rogers, Brookhaven National Laboratory, Instrumentation Division (amplifier IO 449-1; pulse sequencer for digitizer, computer, flashlamp, amplifier, and laser syn-

chronization IO 445-1 and IO 445-2; PT1 xenon lamp-pulse controller IO 441-1).

The CAMAC-controlled digitizer was manufactured by LeCroy Research Systems Corp. of Spring Valley, NY (200 megasample transient recorder TR8828B with memory MM8104). The CAMAC interface with DMA data transfer capability to our DEC 11/23 computer was manufactured by Jorway Corp. of Westbury, NY (CAMAC interface model 411-2229, crate controller type A1, highway terminator model 51C). The RSX-11M CAMAC driver written by Daniel Curtis of Fermi National Accelerator Laboratory, Batavia, IL was generously supplied by that institution.

Kinetics in the 10^{-8} –1 s time range were measured by recording 50 lamp pulse profiles *without* photoexciting the sample followed by 50 profiles *with* sample excitation. The results were ratioed and used to calculate $\Delta A(t)$ due to picosecond photoexcitation. Groups of these 100 laser-shot cycles were further averaged up to 99 times as needed (see below).

In some of the figures, approximate excited-state absorption spectra are presented along with the ground-state spectra. These excited-state spectra were calculated by adding a minimum amount of ground-state absorbance to the difference spectra to produce nonnegative and smoothly varying extinction coefficients (ϵ) across the region of the ground-state absorption. The results are therefore limiting excited-state ϵ 's.

The photoexcitation wavelength was 532 nm for complexes II, III, and IV and 650 nm for complex I. The samples were held at room temperature in argon-filled chambers during experimentation. The main reservoir was magnetically stirred to create regions of high and low velocity. Glass tubes transferred sample solution continuously from the high- to the low-pressure regions of the reservoir and a 2-mm path length sample cell was inserted into this transfer line. In this way each ΔA measurement was made on a fresh sample.

Luminescence lifetime measurements were made following photoexcitation at 532 nm by detecting the front surface emission of a sample solution. The detector was a Varian VPM-152 photomultiplier with 350 ps risetime. Both 7844 and 7904 Tektronix oscilloscopes were used with 7A19 amplifiers to record the emission lifetimes. Instrument-response-limited lifetimes were 1.1 and 1.4 ns, respectively, for the 7904 and 7844 oscilloscopes.

Relative luminescence quantum yields (Φ_{em}) were measured by the method of Demas and Crosby¹⁰ by using an instrument constructed at MSU.¹¹ The quantum yield standard was $Mo_2Cl_4(PBu_3)_4$, which has a reported $\Phi_{em} = 0.013$ with 542-nm excitation, in 2-methylpentane solution at room temperature.³⁸

Sample Preparation. $(TBA)_2[Re_2Cl_8]$ ($TBA = Bu_4N^+$),¹² $K_4[Mo_2Cl_8]$,¹³ $Mo_2Cl_4(CH_3CN)_4$,¹⁴ and $Mo_2Cl_4(PBu_3)_4$ ¹⁵ ($Bu = n-C_4H_9$) were prepared according to the published procedures and stored under Ar. Elemental analysis was performed by Galbraith Inc.

Acetonitrile and methylene chloride (Burdick and Jackson) were degassed with seven freeze–pump–thaw cycles on a high vacuum ($<10^{-5}$ torr) line and stored under vacuum over activated molecular sieves (3- \AA for CH_3CN , 4- \AA for CH_2Cl_2). Samples for both transient absorption and emission quantum yield experiments were prepared by transferring solvent by flask-to-flask vacuum distillation directly into the sample cell containing the compound to be examined. Solutions were further degassed with no fewer than three freeze–pump–thaw cycles and then blanketed with one atmosphere of purified Ar. Absorption spectra of the samples were recorded in the flow cell prior to and following picosecond measurements in order to assess the extent of photochemical decomposition which, in all cases to be described, was negligible.

Results and Discussion

$(TBA)_2[Re_2Cl_8]$ (I) in CH_3CN . Complex I exhibits a $\delta^2 \rightarrow {}^1(\delta\delta^*)$ absorption maximum at 682 nm and a broad, nonmirror image emission band maximizing at 780 nm.³⁸ The luminescence lifetime of I in CH_3CN is 140 ns, and a transient absorption maximum at 390 nm has been found to decay with the same lifetime.¹⁶ The luminescence has been proposed to arise from a ${}^1(\delta\delta^*)$ excited state in which the molecule has relaxed to a staggered geometry. The

(10) Demas, J. N.; Crosby, G. A. *J. Phys. Chem.* **1971**, *75*, 991.

(11) Mussell, R. D.; Nocera, D. G., submitted for publication in *J. Am. Chem. Soc.*

(12) Barder, T. J.; Walton, R. A. *Inorg. Chem.* **1982**, *21*, 2510.

(13) Brenic, J. V.; Cotton, F. A. *Inorg. Chem.* **1970**, *9*, 351.

(14) San Filippo J., Jr.; Sniadoch, H. J.; Grayson, R. L. *Inorg. Chem.* **1974**, *13*, 2121.

(15) Glicksman, H. D.; Hamer, A. D.; Smith, T. J.; Walton, R. A. *Inorg. Chem.* **1976**, *15*, 2205.

(16) Flemming, R. H.; Geoffroy, G. L.; Gray, H. B.; Gupta, A.; Hammond, G. S.; Kligler, D. S.; Miskowski, V. M. *J. Am. Chem. Soc.* **1976**, *98*, 48.

(9) Winkler, J. R.; Netzel, T. L.; Creutz, C.; Sutin, N., submitted for publication.

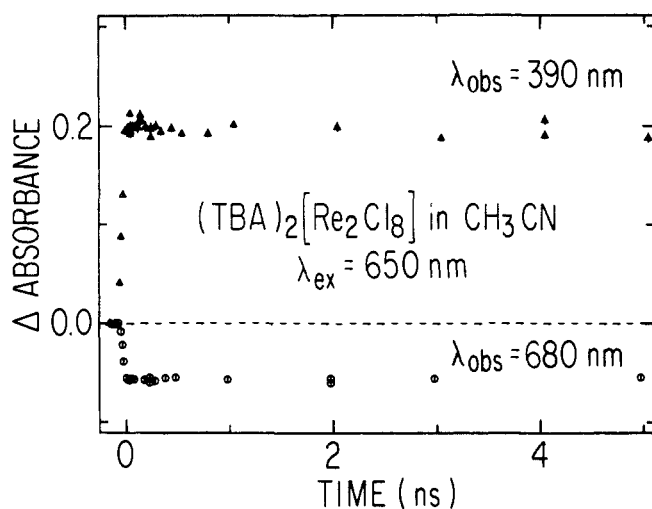


Figure 3. Transient kinetics for $(\text{TBA})_2[\text{Re}_2\text{Cl}_8]$ in CH_3CN (1.6 mM) recorded at 680 nm (O) and 390 nm (Δ) with 650-nm laser excitation.

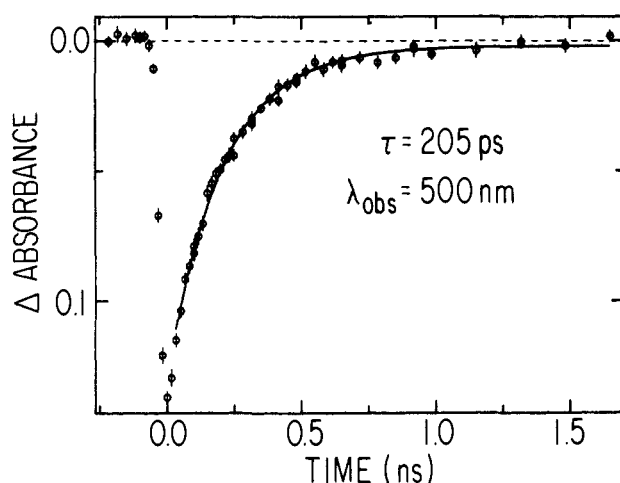
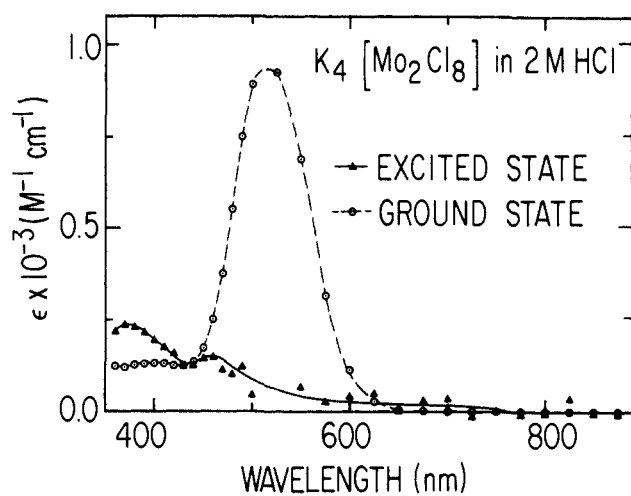


Figure 4. Excited- and ground-state absorption spectra (upper) and kinetics (lower) for $\text{K}_4[\text{Mo}_2\text{Cl}_8]$ in 2 M HCl (3.5 mM) recorded with 532-nm laser excitation. Upper: excited-state absorption spectrum (Δ) generated by addition of 18% of the ground-state spectrum (O) to the $t = 50$ ps difference spectrum. Lower: kinetics recorded at 500 nm. The solid line is a single exponential function with a decay lifetime of 205 ps.

390-nm transient absorption feature has been assigned to a ligand to metal charge-transfer (LMCT) transition. The kinetics data in Figure 3 demonstrate that the long-lived excited state of I is formed less than 20 ps after excitation at 650 nm. Accepting then the proposal that this transient is the $^1(\delta\delta^*)$ state of a staggered (D_{4d}) $[\text{Re}_2\text{Cl}_8]^{2-}$ molecule, we must conclude that the rotation

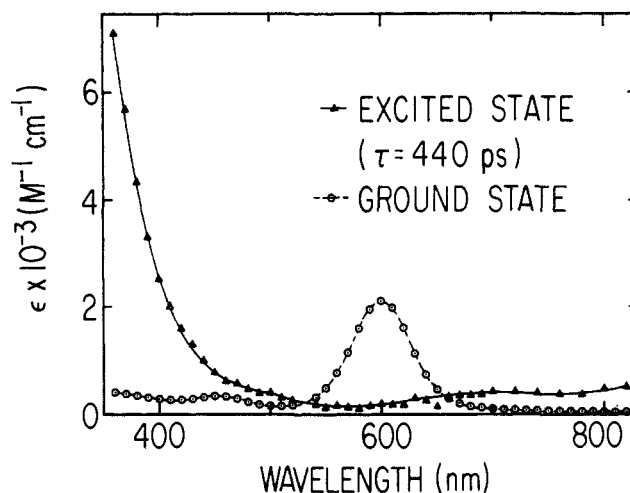
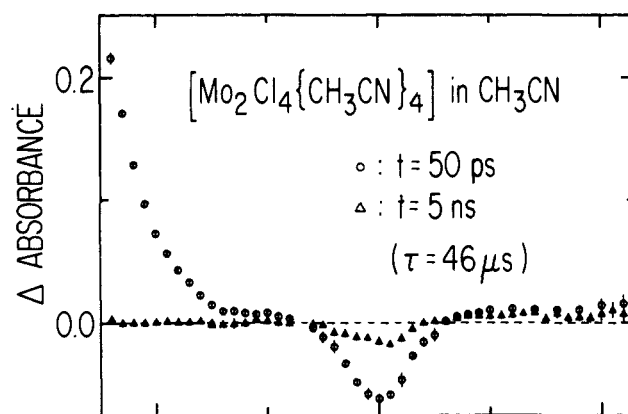


Figure 5. Transient difference spectra (upper) and ground- and excited-state absorption spectra (lower) for $\text{Mo}_2\text{Cl}_4(\text{CH}_3\text{CN})_4$ in CH_3CN (4 mM), recorded with 532-nm laser excitation. Upper: difference spectra recorded 50 ps (O) and 5 ns (Δ) after excitation. Lower: excited-state absorption spectrum (Δ) generated by addition of 4% of the ground-state spectrum (O) to the $t = 50$ ps difference spectrum.

about the metal-metal axis to produce this state is complete in <20 ps.

$\text{K}_4[\text{Mo}_2\text{Cl}_8]$ (II) in 2 M HCl. The kinetics data recorded in the region of the 515-nm $\delta^2 \rightarrow ^1(\delta\delta^*)$ absorption maximum of II (bottom, Figure 4) reveal only one kinetically important excited state. This state is formed in less than 20 ps and has a lifetime of 205 ps. The ground- and excited-state spectra for complex II are shown in the upper half of Figure 4. The 390-nm LMCT transition present in the $^1(\delta\delta^*)$ state of $[\text{Re}_2\text{Cl}_8]^{2-}$ is most likely blue-shifted out of our observation window in $[\text{Mo}_2\text{Cl}_8]^{4-}$, as is the case for LMCT transitions from the δ^2 ground states of these complexes.^{3d,4b}

$\text{Mo}_2\text{Cl}_4(\text{CH}_3\text{CN})_4$ (III) in CH_3CN . In III, four CH_3CN ligands replace four Cl^- ligands of II. This substitution should reduce the electron density on the metals and shift the LMCT bands to lower energy. The $\delta^2 \rightarrow ^1(\delta\delta^*)$ absorption band of III maximizes at 600 nm, 2750 cm^{-1} lower than in II. Transient kinetics reveal the presence of two species with lifetimes of 440 ps and 46 μs . Difference spectra for III in CH_3CN are shown for two delay times (50 ps and 5 ns) in the upper portion of Figure 5. Importantly, the first transient exhibits very strong absorption for $\lambda \lesssim 370$ nm. The excited-state spectrum in the lower part of Figure 5 indicates that $\epsilon_{\text{max}} > 7000 \text{ M}^{-1} \text{ cm}^{-1}$. By analogy with I, this near-UV absorption most likely arises from LMCT transitions of the $^1(\delta\delta^*)$ excited state.

Complex III, like complexes I and II, has no steric barrier to rotation about the M-M bond. As was the case for complexes I and II, only one $^1(\delta\delta^*)$ MMCT state is seen by transient absorption spectroscopy, and it is formed in <20 ps. It is probable

therefore that complexes I–III all show only staggered and not eclipsed $^1(\delta\delta^*)$ states.

The difference spectrum recorded 5 ns after excitation of III (Figure 5) reveals a second transient species that decays back to the ground state with a lifetime of 46 μs . No luminescence from III has been detected at wavelengths shorter than 1100 nm. If this long-lived transient corresponds to an excited state lying $>10000\text{ cm}^{-1}$ above the ground state, then the upper limit of 10^{-5} on the luminescence yield places an upper limit of 1 s^{-1} on the radiative rate constant for the state.¹⁷ This value is some 3–5 orders of magnitude smaller than typical radiative rate constants for $T_1 \rightarrow S_0$ transitions in second- and third-row transition-metal complexes.¹⁸ The likelihood therefore is that this long-lived transient species is either (i) an excited state below 10000 cm^{-1} or (ii) a structurally distorted derivative of III.

The $^3(\delta\delta^*)$ excited state of III in the eclipsed configuration is believed to lie $\sim 5000\text{ cm}^{-1}$ above the ground state⁶ and is a candidate for this long-lived transient. The potential energy minimum for the $^3(\delta\delta^*)$ state of III, a complex with relatively small ligands, however, will be found in the staggered configuration.¹⁹ In this geometry, the $^3(\delta\delta^*)$ and δ^2 states are nearly degenerate⁶ and, by virtue of the significant spin-orbit coupling constant expected for Mo(II),²³ quite strongly coupled. The $^3(\delta\delta^*)_{\text{staggered}} \rightarrow \delta^2_{\text{staggered}}$ transition in III is analogous to intersystem crossing transitions in organic biradicals. The rate constants for these processes in organic molecules with relatively little spin-orbit coupling, though, are typically 1–2 orders of magnitude greater than the value of $2.2 \times 10^4\text{ s}^{-1}$ found for the decay of the final transient in III.²⁴ These considerations suggest that the long-lived transient in III does not arise from a $^3(\delta\delta^*)$ excited state.

Alternatively, the long-lived transient species could be a structurally distorted form of III. One possibility is a $\delta^2_{\text{staggered}}$ species, though the 46 μs lifetime appears far too long for the staggered \rightarrow eclipsed transformation. More likely is a major structural distortion of the complex which includes addition or loss of CH_3CN ligands. A confacial bioctahedral complex, for example, could be prepared by bending three terminal ligands to bridging positions and filling the vacant coordination site with CH_3CN . Whatever the precise form of the distorted species, the 46- μs relaxation would correspond to reconstruction of the original quadruply bonded molybdenum dimer.²⁵ The small spectral differences between III and its long-lived transient are consistent with this assignment.

$\text{Mo}_2\text{Cl}_4(\text{PBu}_3)_4$ (IV) in CH_2Cl_2 . The steric bulk of the phosphine ligands in IV distinguishes this complex from I–III in that the potential energy with respect to rotation about the metal–metal bond is expected to be at a minimum near the eclipsed configuration for all bound electronic states of the molecule. The mirror image absorption and emission spectra of IV, and congeners with different halide and phosphine ligands,^{3a,8} support this expectation. In contrast to the 10^{-4} quantum yield and 140-ns luminescence lifetime of I in CH_3CN , the reported quantum yield and lifetime

(17) This rate constant was calculated from the expression $\Phi_{\text{em}} = \Phi_{\text{f}}\tau_{\text{obsd}}k_{\text{r}}$, where Φ_{em} is the luminescence quantum yield ($<10^{-5}$), Φ_{f} is the yield of formation of the luminescent state (~ 0.2 , based on estimate of transient bleach), τ_{obsd} is the observed lifetime (46 μs), and k_{r} is the radiative rate constant.

(18) (a) Maverick, A. W.; Najdzionek, J. S.; MacKenzie, D.; Nocera, D. G.; Gray, H. B. *J. Am. Chem. Soc.* **1983**, *105*, 1878. (b) Caspar, J. V.; Meyer, T. J. *J. Am. Chem. Soc.* **1983**, *105*, 5583.

(19) This conclusion is based on the analogy between the $^3(\delta\delta^*)$ state and triplet states of simpler, well-characterized molecules. Examples are the $^3(\sigma\sigma^*)$ state of H_2 and the $^3(\pi\pi^*)$ state of C_2H_4 . In the former case, the energy of the $^3(\sigma\sigma^*)$ state increases monotonically as the internuclear distances decreases from infinity.^{20–22} The energy of the $^3(\pi\pi^*)$ state of ethylene is a sinusoidal function of the dihedral angle between the two CH_2 planes with a period of π and a minimum at $\pi/2$.²²

(20) Coulson, C. A.; Fischer, I. *Phil. Mag.* **1949**, *40*, 386.

(21) Wilson, C. W.; Goddard, W. A. *Theor. Chim. Acta* **1972**, *26*, 195, 211.

(22) Salem, L.; Rowland, C. *Agnew. Chem., Int. Ed. Engl.* **1972**, *11*, 92.

(23) Figgis, B. N. *Introduction to Ligand Fields*; Interscience: New York, 1966; p 60.

(24) *Diradicals*; Borden, W. T., Ed.; Wiley-Interscience: New York, 1982.

(25) A similarly long lifetime has been reported for the transient decay in $\text{Mo}_2(\text{O}_2\text{CCF}_3)_4$ and attributed to a ligand substitution reaction.²⁶

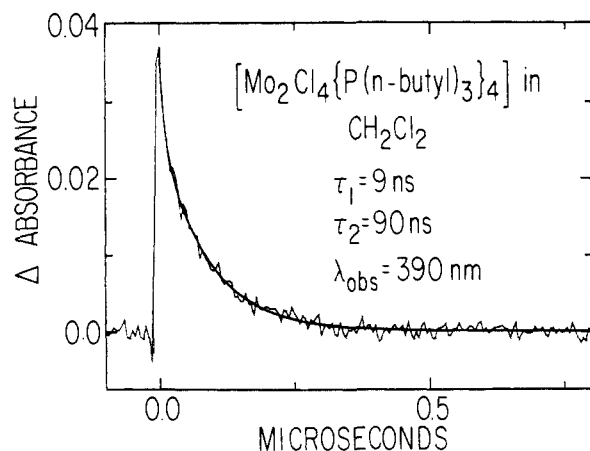


Figure 6. Long time ($>10^{-8}\text{ s}$) transient kinetics for $\text{Mo}_2\text{Cl}_4(\text{PBu}_3)_4$ in CH_2Cl_2 (1.7 mM) recorded at 390 nm following 532-nm laser excitation. The smooth line is a least-squares fit to the data with a biexponential function that decays with lifetimes of 9 and 90 ns.

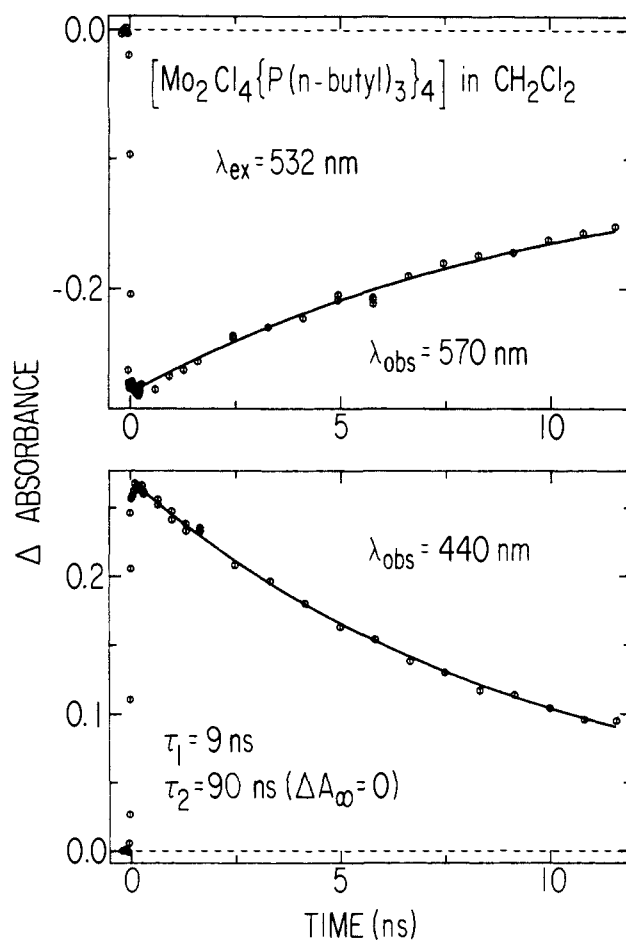


Figure 7. Transient kinetics for $\text{Mo}_2\text{Cl}_4(\text{PBu}_3)_4$ in CH_2Cl_2 (1.5 mM) recorded at 570 (upper) and 440 nm (lower) following 532 nm excitation. The solid line in both plots is a double exponential function with lifetimes of 9 and 90 ns that decays to $\Delta A = 0$ as $t \rightarrow \infty$.

of IV in 2-methylpentane are 0.013 and 16 ns, respectively.^{3b} The factor of 10^3 difference in radiative rate constants for the luminescent transitions in I and IV is attributable to the inability of IV to rotate to a staggered configuration in the $^1(\delta\delta^*)$ excited state.

The luminescence lifetime of complex IV in CH_2Cl_2 , measured after excitation with a ~ 25 -ps pulse of 532-nm light, is 9.0 ± 0.4 ns. The kinetics recorded by transient absorption at 390, 440, and 570 nm (Figures 6 and 7) however show two decay lifetimes, 9 and 90 ns. Since the luminescence spectrum of complex IV is the mirror image of the $\delta^2 \rightarrow ^1(\delta\delta^*)$ absorption profile, and since the luminescence lifetime is 9 ns, the first transient must corre-

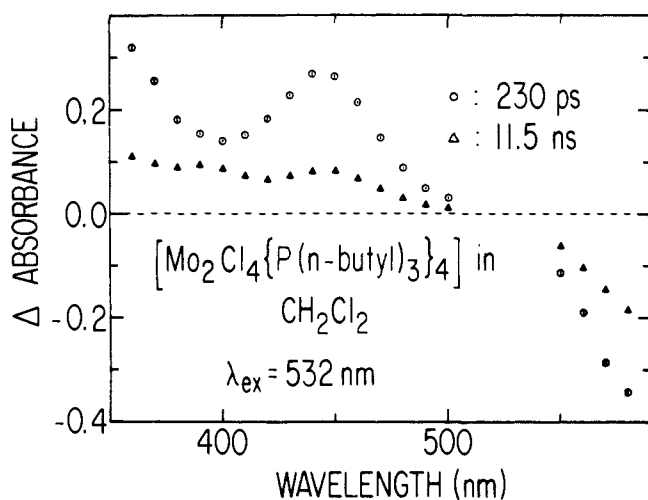


Figure 8. Transient difference spectra for $\text{Mo}_2\text{Cl}_4(\text{PBu}_3)_4$ in CH_2Cl_2 (1.5 mM) recorded 230 ps (O) and 11.5 ns (Δ) after 532-nm laser excitation.

spond to the eclipsed $^1(\delta\delta^*)$ excited state. Three possibilities present themselves for the long-lived (90 ns) transient species: (i) the low-lying (ca. $5,000\text{ cm}^{-1}$) $^3(\delta\delta^*)$ state; (ii) an electronic excited state of IV that lies only slightly lower in energy than the $^1(\delta\delta^*)$ state but carries very little oscillator strength to the ground state; and (iii) a highly distorted chemical intermediate form of IV.

Two transient difference spectra of complex IV in CH_2Cl_2 are shown in Figure 8. The 230-ps spectrum, corresponding to the $^1(\delta\delta^*)$ state, exhibits a moderately intense absorption maximum at 440 nm and absorption rising into the near-UV. This near-UV absorption ($\lambda > 400\text{ nm}$) probably arises from charge-transfer transitions. The identity of the 440-nm absorption band in IV is less clear. The extinction coefficient of this band is ca. $2000\text{ M}^{-1}\text{ cm}^{-1}$ (ES1, upper portion of Figure 9). This value clearly indicates a spin and dipole allowed transition but does not help discriminate between CT and metal-localized excitations. That no directly analogous feature appears in the $^1(\delta\delta^*)$ state spectrum of III may imply that the band arises from charge-transfer transitions involving the phosphine ligands. Alternatively, this band could be a metal-localized transition that is blue-shifted in III and obscured by the low energy tail of the proposed charge-transfer absorption. Assuming D_{4h} selection rules, five dipole-allowed, one-electron, metal-localized excitations can arise from a $^1(\delta\delta^*)$ excited state: $\delta \rightarrow \delta^*$; $\pi \rightarrow \pi^*$; $\pi \rightarrow \delta'(x^2 - y^2)$; $\delta^* \rightarrow \pi^*$; and $\pi \rightarrow \delta$. These transitions will produce, respectively, $^1A_{1g}(\delta\delta^2)$, $^1A_{1g}(\pi^3\delta\delta^*\pi^*)$, $^1E_g(\pi^3\delta\delta^*\delta')$, $^1E_g(\delta\pi^*)$, and $^1E_g(\pi\delta^*)$ states. The level arising from the 440-nm absorption must lie ca. $39,000\text{ cm}^{-1}$ above the ground state, and calculations suggest that, of the five metal-localized excitations, the $\delta^* \rightarrow \pi^*$ excitation is the most plausible assignment for this feature.^{4b-d} The data, at present, do not permit an unequivocal assignment of the 440-nm band, but phosphine related CT transitions or $^1A_{2u}(\delta\delta^*) \rightarrow ^1E_g(\delta\pi^*)$ excitations appear to be the best candidates.

By 11.5 ns the $^1(\delta\delta^*)$ state is 70% relaxed, and features corresponding to the 90 ns-lived species appear in the transient difference spectrum (Figure 8). Specifically, an absorption feature maximizing at $\sim 390\text{ nm}$, which is *not* present in the $^1(\delta\delta^*)$ spectrum, appears in the 11.5-ns spectrum. This new absorption feature clearly demonstrates the presence of a different transient species, but the overlapping absorption from the partially relaxed $^1(\delta\delta^*)$ state prevents reliable determination of its difference spectrum. This difficulty, was eliminated, however, by changing to a solvent in which IV exhibits significantly different photo-physics.

$\text{Mo}_2\text{Cl}_4(\text{PBu}_3)_4$ (IV) in CH_3CN . Upon changing the solvent from methylene chloride to acetonitrile the luminescence quantum yield of IV drops by a factor of 45 while the lifetime drops by a factor of 2.2 down to $4.0 \pm 0.3\text{ ns}$. That the lifetime and quantum yield decrease by different factors indicates a change in radiative rate constants for the emitting states in the two solvents. Nevertheless, the kinetics data in Figure 10 demonstrate

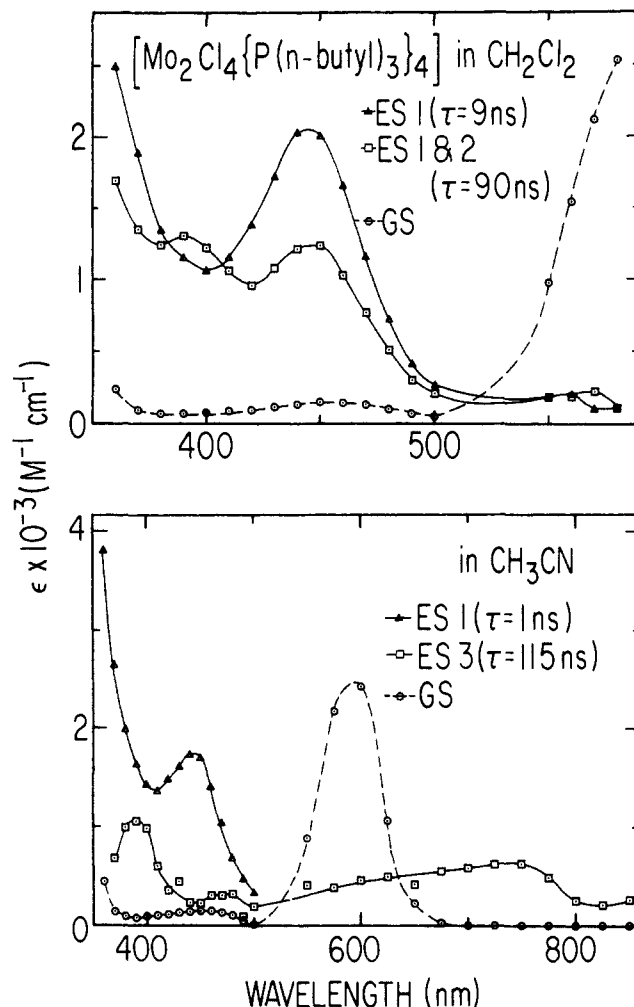


Figure 9. Ground- and excited-state spectra of $\text{Mo}_2\text{Cl}_4(\text{PBu}_3)_4$ in CH_2Cl_2 (upper) and CH_3CN (lower). Upper: spectra generated by addition of 32% (Δ) and 18% (\square) of the ground-state spectrum (O) to the $t = 230\text{ ps}$ and $t = 11.5\text{ ns}$ difference spectra, respectively. Lower: spectra generated by addition of 38% (Δ) and 8% (\square) of the ground-state spectrum (O) to the $t = 70\text{ ps}$ and $t = 11.5\text{ ns}$ difference spectra, respectively.

that a long-lived ($\tau = 115\text{ ns}$), nonemitting transient is produced by 532-nm excitation of IV in CH_3CN , as it was in CH_2Cl_2 .

Figure 11 presents kinetics data in the 10^{-11} – 10^{-8} s time range. At 440 nm the data are well fit with two decay lifetimes of 1 and 4 ns. The latter is the same as the emission lifetime measured with our 1-ns resolution emission detection equipment. It is likely that the 1 ns-lived transient also emits, but we could not detect this emission in the presence of the 4-ns emission component. All three relaxation processes ($\tau = 1, 4,$ and 115 ns) can be observed by transient absorption at 580 nm.

Difference spectra of the three transients are presented in Figure 12. The first two spectra ($t = 70\text{ ps}$ and 3 ns) are very similar, with both exhibiting strong CT absorptions in the near-UV and absorption maxima near 440 nm. These features match those found in methylene chloride and are characteristic of $^1(\delta\delta^*)$ MMCT states (vide supra). Comparison of the spectra of the first excited state (ES1) of complex IV in these two solvents (Figure 9) shows that the strong CT absorption of the $^1(\delta\delta^*)$ state red-shifts on going to the more polar solvent, CH_3CN . The 1-ns decay of the first transient to the second in CH_3CN probably corresponds to a nuclear relaxation of the $^1(\delta\delta^*)$ state. The extent of this nuclear rearrangement is not known, but the presence of the bulky PBu_3 ligands is likely to prevent formation of a completely staggered $^1(\delta\delta^*)$ state.

The difference spectrum of the 115-ns-lived transient was recorded at 11.5 ns and clearly shows an absorption feature at 390 nm as well as the absence of CT absorption in the near UV (λ

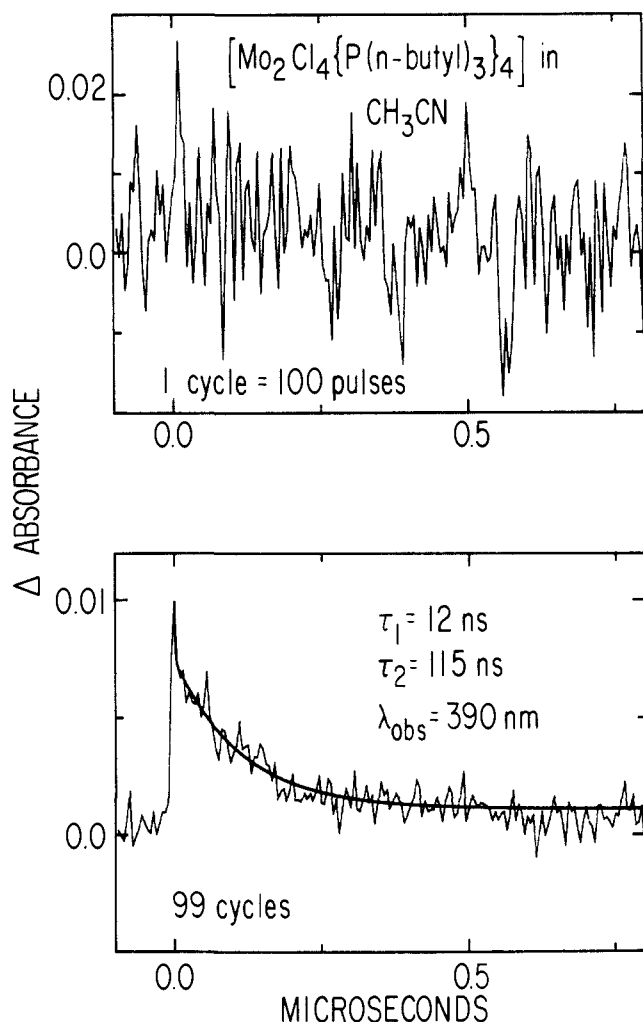


Figure 10. Long time ($>10^{-8}$ s) transient kinetics for $\text{Mo}_2\text{Cl}_4(\text{PBu}_3)_4$ in CH_3CN (0.6 mM) recorded at 390 nm following 532-nm laser excitation. The upper plot is the signal resulting from one cycle of 50 blank and 50 excitation traces, and the lower plot is the signal resulting from the average of 99 such cycles. The solid line in the lower plot is a biexponential function that decays with lifetimes of 12 and 115 ns.

> 350 nm). Both observations agree with the results for complex IV in CH_2Cl_2 (see Figure 8). In addition to the 390-nm absorption band, the approximate absorption spectrum for this transient (Figure 9) displays weak, broad absorption near 750 nm. The spectral data do not permit a definitive assignment of the long-lived transient and arguments in support of each of three distinct possibilities can be formulated.

The most obvious assignment for the long-lived transient is the $^3(\delta\delta^*)$ excited state of IV, which has been estimated at 5200 cm^{-1} above the ground state.⁶ One argument against such an assignment derives from the luminescence properties of a series of $\text{Mo}_2\text{Cl}_4(\text{PR}_3)_4$ ($\text{R} = \text{Me}, \text{Et}, \text{Pr}, \text{Bu}$) molecules.⁸ The PMe_3 complex has a luminescence quantum yield of 0.26 and a lifetime of 140 ns. In the PEt_3 , PPr_3 , and PBu_3 (IV) complexes, the room temperature quantum yields and lifetimes are an order of magnitude smaller. Our results demonstrate that in IV the reduced yield and lifetime result from nonradiative decay of the luminescent $^1(\delta\delta^*)$ state to the long-lived transient species. A similar process appears likely in the PPr_3 and PEt_3 complexes but unlikely in the PMe_3 complex. The perturbation resulting from replacement of PMe_3 by PEt_3 , PPr_3 , or PBu_3 seems insufficient to significantly alter the $^1(\delta\delta^*) \rightarrow ^3(\delta\delta^*)$ intersystem crossing rate. These considerations, though not conclusive, point to alternative assignments for the final transient in IV.

If the long-lived transient in IV arises from an excited state lying just below the $^1(\delta\delta^*)$, then the best candidate is the $^3\text{E}_g(\pi\delta^*)$ state. The ab initio calculation of $\text{Re}_2\text{Cl}_8^{2-}$ places this excited state at the same energy as the $^1\text{A}_{2u}(\delta\delta^*)$ state (Table I). Furthermore,

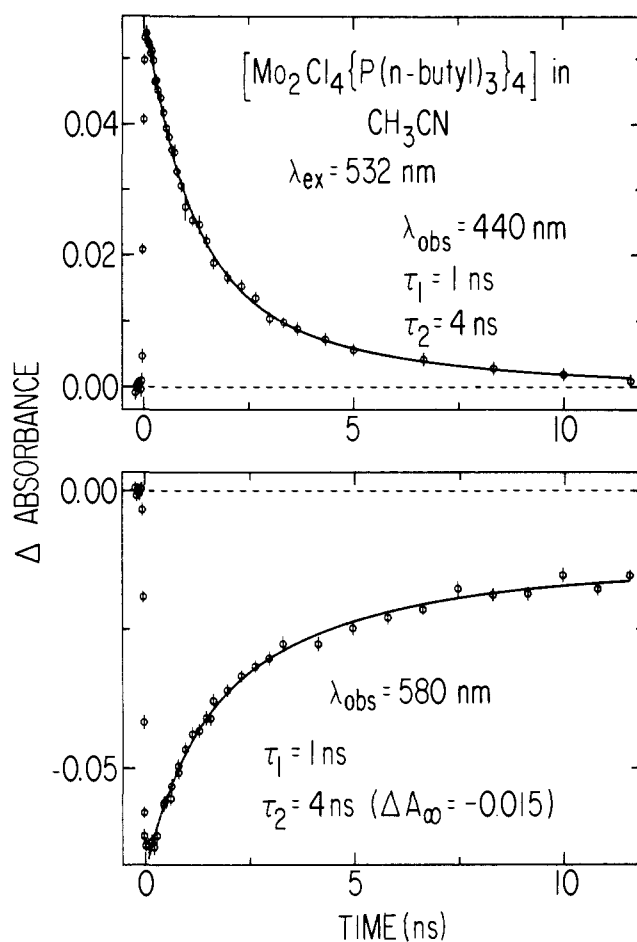


Figure 11. Transient kinetics for $\text{Mo}_2\text{Cl}_4(\text{PBu}_3)_4$ in CH_3CN (0.4 mM) recorded at 440 (upper) and 580 nm (lower) following laser excitation at 532 nm. The solid line in the upper plot is a biexponential function that decays with lifetimes of 1 and 4 ns. The solid line in the lower plot is a biexponential function that decays with lifetimes of 1 and 4 ns and approaches $\Delta A = -0.015$ as $t \rightarrow \infty$.

spin and dipole forbidden $^1\text{A}_{1g} \rightarrow ^3\text{E}_g$ transitions would be quite difficult to detect beneath the low-energy tail of the intense $\delta \rightarrow \delta^*$ absorption profile. The presence of a close-lying excited state can easily account for the luminescence properties in $\text{Mo}_2\text{Cl}_4(\text{PR}_3)_4$ complexes. Changing R from Me to a longer chain alkyl could sufficiently perturb a nearly degenerate pair of states [$^1(\delta\delta^*)$ and $^3(\pi\delta^*)$] to invert their ordering. It is possible, then, that the $^1(\delta\delta^*)$ state lies below the $^3(\pi\delta^*)$ state when $\text{R} = \text{Me}$, while the reverse order would obtain when $\text{R} = \text{Bu}$. The luminescence lifetimes of the four $\text{Mo}_2\text{Cl}_4(\text{PR}_3)_4$ molecules ($\text{R} = \text{Me}, \text{Et}, \text{Pr}, \text{Bu}$) converge to nearly identical values at low temperature (77 K),^{8b} suggesting that the nonradiative transition from the $^1(\delta\delta^*)$ state in IV is a thermally activated process. This observation is somewhat difficult to rationalize in terms of a $^3(\pi\delta^*)$ assignment for the long-lived transient. The $^1(\delta\delta^*)$ and $^3(\pi\delta^*)$ states are unlikely to be greatly distorted relative to one another, and a weak coupling, temperature-independent, nonradiative transition²⁷ between the two would be more probable. Another difficulty with a $^3(\pi\delta^*)$ assignment for the long-lived transient in IV is its absorption spectrum, which displays only a weak band maximizing at 390 nm and a broad feature at 750 nm. A triplet state lying just below ($<3000\text{ cm}^{-1}$) the $^1(\delta\delta^*)$ state would be expected to display strong CT absorption features at roughly the same energy as those of the $^1(\delta\delta^*)$ state.²⁸ If this expectation is correct, then

(26) Miskowski, V. M.; Twarowski, A. J.; Fleming, R. H.; Hammond, G. S.; Kliger, D. S. *Inorg. Chem.* 1978, 17, 1056.

(27) Englman, R.; Jortner, J. *J. Mol. Phys.* 1970, 18, 145.

(28) This prediction is based upon the assumptions that the singlet-triplet energy gap for these CT states is $\sim 3000\text{ cm}^{-1}$ and that CT states of the proper symmetry are available.

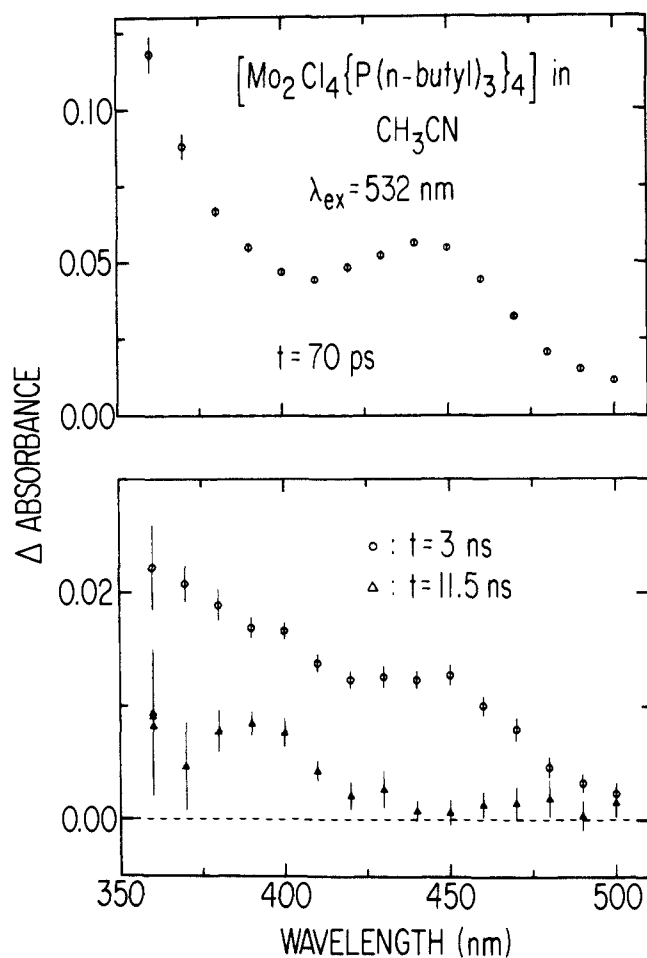


Figure 12. Transient difference spectra for $\text{Mo}_2\text{Cl}_4(\text{PBu}_3)_4$ in CH_3CN (0.4 mM) recorded 70 ps (O, upper), 3 ns (O, lower), and 11.5 ns (Δ , lower) after 532-nm laser excitation.

our failure to observe CT absorption features in the spectrum of the final transient in IV creates two possibilities. Either the assignment of the CT absorption feature in the $^1(\delta\delta^*)$ spectrum is incorrect or the long-lived transient is not a $^3(\pi\delta^*)$ state.

The final possibility for the long-lived transient in IV, a chemical intermediate, is equally difficult to prove and to disprove with the available data. One important component of the driving force to form a distorted intermediate from the $^1(\delta\delta^*)$ state of IV is the relief of steric repulsions. In this regard, an interesting comparison can be drawn between the luminescence decay properties of the $\text{Mo}_2\text{Cl}_4(\text{PR}_3)_4$ series and the cone angles²⁹ of their respective phosphine ligands. The cone angle of PMe_3 is 118° while those of PEt_3 , PPr_3 , and PBu_3 are all approximately 132° .²⁹ As mentioned above, the $^1(\delta\delta^*)$ state of $\text{Mo}_2\text{Cl}_4(\text{PMe}_3)_4$ appears to decay simply to the ground state, without passing through an intermediate, longer-lived transient. Complexes with PEt_3 , PPr_3 , and PBu_3 ligands, on the other hand, exhibit faster luminescence decay rates and lower quantum yields, and the $^1(\delta\delta^*)$ state of the latter species (IV) decays to a longer-lived nonluminescent transient. The correlation between cone angle and luminescence properties

does therefore argue for the formation of a distorted intermediate from the $^1(\delta\delta^*)$ state of IV. The invariance of the decay rate constant for this transient in CH_2Cl_2 , CH_3CN , and C_6H_{12} ³⁰ indicates that if a distorted intermediate is being formed, it does not involve extensive solvent participation. Beyond this, however, the data offer little insight into possible distorted structures. The broad, weak absorption near 750 nm in the spectrum of this transient might be a remnant of the $\delta^2 \rightarrow ^1(\delta\delta^*)$ absorption band in the undistorted molecule. A resemblance can even be seen between the transient spectrum and that of the staggered β - $\text{Mo}_2\text{Cl}_4(\text{dmpe})_2$ ($\text{dmpe} = 1,2$ -bis(dimethylphosphino)ethane) molecule, in which the intensity of the $\delta^2 \rightarrow ^1(\delta\delta^*)$ absorption band is greatly diminished.⁶ Speculation as to the structure of a distorted intermediate as well as a firm assignment for the long-lived transient, however, must await further experimental evidence.

Summary

A single excited state is detected by transient absorption spectroscopy following picosecond laser excitation of the $\delta^2 \rightarrow ^1(\delta\delta^*)$ transitions in $[\text{Re}_2\text{Cl}_8]^{2-}$ (I) and $[\text{Mo}_2\text{Cl}_8]^{4-}$ (II). In both cases the transient is formed in less than 20 ps and decays cleanly to the ground state. If the assertion is valid that the $^1(\delta\delta^*)$ states of these molecules prefer a staggered geometry, then the eclipsed-to-staggered conformation change is completed within 20 ps of excitation. The lifetime of the $^1(\delta\delta^*)$ state of $\text{Mo}_2\text{Cl}_4(\text{C}_6\text{H}_5\text{CN})_4$ (III) in CH_3CN is 440 ps, but 532-nm excitation of this molecule also produces a much longer lived ($\tau = 46 \mu\text{s}$) transient. This species is probably a distorted derivative of III.

Difference spectra of $\text{Mo}_2\text{Cl}_4(\text{PBu}_3)_4$ (IV) in CH_2Cl_2 reveal the presence of two transient species following picosecond-laser excitation. The shorter lived transient ($\tau = 9 \text{ ns}$) decays with the same lifetime as the luminescence and must arise from the $^1(\delta\delta^*)$ excited state. The second transient decays with a lifetime of 90 ns. A definitive assignment for this species is not possible at present, but the three most likely candidates are (i) the $^3(\delta\delta^*)$ state, (ii) the $^3(\pi\delta^*)$ excited state, or (iii) a distorted chemical intermediate. Regardless of the precise nature of this transient, its existence is likely to have important consequences for the bimolecular photochemical reactivity of IV.

We are continuing our transient spectroscopic investigations of quadruply bonded transition-metal dimers. With a broader data base from molecules with different ligands and metal centers, it might be possible to resolve some of the questions raised in this work and to construct a model that adequately describes the varied excited-state dynamics of this interesting class of molecules.

Acknowledgment. This research was carried out at Brookhaven National Laboratory under contract DE-AC02-76CH00016 with the U.S. Department of Energy and supported by its Division of Chemical Sciences, Office of Basic Energy Sciences. D.G.N. gratefully acknowledges financial support from the AMAX Foundation, Research Corporation, and the Camille and Henry Dreyfus Foundation. It is a pleasure to acknowledge helpful discussions with N. Sutin and H. B. Gray. We are grateful to I.-J. Chang (MSU) for the preparation of some compounds used in this study.

Registry No. 1, 19584-24-8; 11, 34767-26-5; 111, 51731-46-5; IV, 38832-72-3.

(29) Tolman, C. A. *Chem. Rev.* **1977**, *77*, 313.

(30) The behavior of IV in cyclohexane is quite similar to that in methylene chloride.